

## Levenberg-Marquardt optimised neural networks for trajectory tracking of autonomous ground vehicles

Article (Published Version)

Al-Mayyahi, Auday Basheer Essa, Wang, Weiji and Birch, Philip (2015) Levenberg-Marquardt optimised neural networks for trajectory tracking of autonomous ground vehicles. *International Journal of Mechatronics and Automation*, 5 (2/3). pp. 140-153. ISSN 2045-1067

This version is available from Sussex Research Online: <http://sro.sussex.ac.uk/id/eprint/61718/>

This document is made available in accordance with publisher policies and may differ from the published version or from the version of record. If you wish to cite this item you are advised to consult the publisher's version. Please see the URL above for details on accessing the published version.

### **Copyright and reuse:**

Sussex Research Online is a digital repository of the research output of the University.

Copyright and all moral rights to the version of the paper presented here belong to the individual author(s) and/or other copyright owners. To the extent reasonable and practicable, the material made available in SRO has been checked for eligibility before being made available.

Copies of full text items generally can be reproduced, displayed or performed and given to third parties in any format or medium for personal research or study, educational, or not-for-profit purposes without prior permission or charge, provided that the authors, title and full bibliographic details are credited, a hyperlink and/or URL is given for the original metadata page and the content is not changed in any way.

---

## Levenberg-Marquardt optimised neural networks for trajectory tracking of autonomous ground vehicles

---

Auday Al-Mayyahi\*, Weiji Wang and Phil Birch

School of Engineering and Informatics,  
Department of Engineering and Design,  
University of Sussex, Brighton, UK  
Email: auday.almayyahi@sussex.ac.uk  
Email: W.J.Wang@sussex.ac.uk  
Email: P.M.Birch@sussex.ac.uk

\*Corresponding author

**Abstract:** Trajectory tracking is an essential capability of robotics operation in industrial automation. In this article, an artificial neural controller is proposed to tackle trajectory-tracking problem of an autonomous ground vehicle (AGV). The controller is implemented based on fractional order proportional integral derivative (FOPID) control that was already designed in an earlier work. A non-holonomic model type of AGV is analysed and presented. The model includes the kinematic, dynamic characteristics and the actuation system of the VGA. The artificial neural controller consists of two artificial neural networks (ANNs) that are designed to control the inputs of the AGV. In order to train the two artificial neural networks, Levenberg-Marquardt (LM) algorithm was used to obtain the parameters of the ANNs. The validation of the proposed controller has been verified through a given reference trajectory. The obtained results show a considerable improvement in term of minimising trajectory tracking error over the FOPID controller.

**Keywords:** autonomous ground vehicle; AGV; trajectory tracking; artificial neural network; ANN; FOPID controller.

**Reference** to this paper should be made as follows: Al-Mayyahi, A., Wang, W. and Birch, P. (2015) 'Levenberg-Marquardt optimised neural networks for trajectory tracking of autonomous ground vehicles', *Int. J. Mechatronics and Automation*, Vol. 5, Nos. 2/3, pp.140–153.

**Biographical notes:** Auday Al-Mayyahi received his BSc in Electrical Engineering from the University of Basrah, Iraq in 2003. In 2007, he received his MSc in Power and Machine Engineering from the University of Basrah, Iraq. In 2013, he had a scholarship from Iraqi Government to get his PhD in Industrial Automation from the UK. Currently, he is a PhD Researcher in University of Sussex, UK. His current research interests include industrial automation, robotics, and intelligent control systems.

Weiji Wang received his PhD degree from the Oxford University in 1993. Currently, he is a member of faculty in School of Engineering and Design, University of Sussex. His current research interests include automotive dynamics and control, signal processing and vehicle engineering.

Phil Birch completed his PhD at the University of Durham in 1999 on Liquid Crystal Devices in Adaptive Optics. He has worked in industry developing rapid prototyping equipment and optical metrology systems. Since working at the University of Sussex, he has been researching computer generated holograms (CGH), correlation pattern matching, and optical microscopy. He has also worked with industrial partners in image processing, object detection and tracking.

---

### 1 Introduction

In the past two decades, it has been noticed an increased attention in the area of motion control of autonomous ground vehicles (AGVs). The trajectory tracking problem is a typical motion control problem and it is one of the major challenges in robotics. In many applications, AGVs operate autonomously over predefined trajectories to track a given trajectory in an environment. In other words, the AGVs will be enforced using a control methodology to follow a given

trajectory. In the most recent research, many algorithms and control techniques have been proposed to cope with the trajectory tracking problem. Therefore, to solve this problem, it is necessary to have a methodology that allows guiding the AGVs to track the given trajectory from starting to the end of the trajectory. This methodology deals with motion planning that focuses on determining how to move the AGVs along the solution given by the trajectory

algorithm in a way that both kinematic and dynamic characteristics of the AGVs are taken into consideration.

A bibliographic review of some important related work that embraces different approaches of AGV trajectory tracking is provided. Padhy et al. (2010) designed a traditional PID controller for trajectory tracking. The structure and implementation of the PID was simple and yet valid for tracking performance. However, the proposed controller is not sufficient for applications that require high trajectory tracking accuracy. Guo et al. (2014) reported the trajectory tracking controller of closed-loop control structure is derived using an integral back-stepping method to construct a new virtual variable. The Lyapunov theory is utilised to analyse the stability of the proposed tracking controller. Pawlowski et al. (2001) implemented a fuzzy logic for a mobile robot. The kinematic model of the mobile robot was introduced in the implementation. Antonelli et al. (2007) also proposed a fuzzy logic approach to deal with the trajectory tracking problem. In this approach, the input to fuzzy system is represented by approximate information concerning the next bend ahead the vehicle; the corresponding output is the cruise velocity that the vehicle needs to attain in order to safely drive on the path.

Shojaei et al. (2009) presented an adaptive controller for the trajectory tracking of wheeled mobile robots (WMRs) based on a feedback linearisation technique. The adaptive controller was a design based on an input-output feedback linearisation technique to get asymptotically exact cancellation for the uncertainty in the given system parameters. The presented adaptive controller was designed based on the Lyapunov approach. Keighobadi et al. (2010) designed feedback linearisation and fuzzy controllers for the trajectory tracking of a WMR. The linguistic if-then rules of fuzzy controllers are constructed using knowledge and experience of expert humans about variations of input torque with respect to the WMR's position and velocity variables. Jiang and Nijmeijer (1997) proposed a tracking control methodology via time-varying state feedback based on the back-stepping technique. Local and global tracking problem were considered based on initial tracking error which is set arbitrary. Hao et al. (2014) presented a trajectory tracking control methodology base on a fuzzy approach. In this methodology, both kinematic and dynamic were derived using Lagrange's equations.

Xu et al. (2014) designed fuzzy PID controller for trajectory tracking mobile robots. The controller combines between of a PID technique and fuzzy inference system. The paper shows a comparison between traditional PID and the integrated PID-fuzzy control. Liang et al. (2010) proposed an adaptive fuzzy control for trajectory tracking of mobile robot. The proposed method integrated PD controller with the fuzzy controller to make use of full Benefits of both controllers. Xie et al. (2012) integrated a fuzzy control with a slide mode technique to deal with trajectory tracking problem of mobile robots. The slide mode technique implemented based on the kinematic characteristic. On the other side, the fuzzy controller used to solve the constant speed problem.

Fukao et al. (2000) integrated both kinematic controller and a torque controller for the dynamic model of a non-holonomic mobile robot. The adaptive controller for the dynamic model was designed using back-stepping method. The derivative of a torque controller was based on the kinematic controller. Solea et al. (2009) presented a slide mode control strategy for trajectory tracking of a WMR. The strategy implemented in the presence uncertainties, i.e., mass and moment of inertia. Ye (2008, 2013) presented two pieces of research based on neural network technique. The implemented architecture was based on the tracking control of the velocity and orientation of a non-holonomic mobile robot. The first research was based on a PID neural network technique. This technique tracked the velocity and orientation of a non-holonomic mobile robot. The second researched method was based on compound sine function neural networks to track control of a two-wheel driven mobile robot. The sine function implemented in the hidden layer was produced by combining a sine function with a unipolar sigmoid function. In that methodology, the weight values are only adjusted between the nodes in hidden layer and the output nodes, while the weight values between the input layer and the hidden layer are one, that is, constant, without the weight adjustment.

In previous work of the above researchers, there is still room to improve the accuracy of the tracking and the response time. Therefore, in this paper, the contribution can be understood as by introducing a new artificial neural network (ANN) model for obtaining the minimum tracking error and improving the trajectory-tracking response in AGVs. This ANN model is a relative simple module therefore the computational complexity will be low. The new Levenberg-Marquardt (LM) algorithm has been used to optimise the parameters of neural network. The LM algorithm has a stable and fast performance relative to the other traditional algorithms that used for optimisation neural network. The computational complexity of this optimisation algorithm is based on the Jacobian method. The introduced ANN technique shows a remarkable improvement in terms of minimising the trajectory tracking error and the time response in comparison with the state of the art. The architecture of ANN consists of two neural controllers. The first one deals with steering control to enforce the AGV tracking of the give trajectory, whereas, the second ANN deals with tracking a reference velocity to maintain a constant velocity during the movement. The parameters of these two ANN controllers are obtained using LM algorithm, i.e., weights and biases. These simulation results are compared with fractional order proportional integral derivative (FOPID) controller that implemented in an earlier work (Al-Mayyahi et al., 2015).

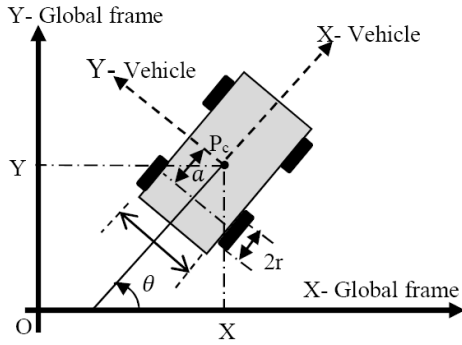
The outline of this article is as follows: In Section 2, the modelling of an autonomous ground vehicle is derived and analysed. This includes kinematic, dynamic characteristics and an actuation system. The explanation of the fractional order systems are described in Section 3. In Section 4, the description of the neural network architecture is given. In addition, four training algorithms are derived and explained

starting from back-propagation algorithm and ending by Levenberg-Marquardt algorithm. The implementation process of the proposed methodology is introduced in Section 5. In Section 6, the obtained results are described and comparisons are conducted to show the significance of ANN optimised by LM algorithm over the fractional order control technique. Finally, in Section 7, conclusions are provided.

## 2 Modelling of an AGV

The modelling for wheeled AGV is described in the following section. This modelling includes analysis for both of the kinematic and dynamic models. The kinematic model describes the motion of the vehicle without considering the forces that cause this motion. In contrast, the dynamic model takes into consideration of the forces that cause the motion. The schematic diagram of the AGV is depicted in Figure 1.

**Figure 1** The schematic diagram of the AGV



### 2.1 Kinematic model

Cartesian coordinates can conduct the kinematic analysis of differentially wheeled autonomous vehicle in a two-dimensional plane. It is assumed that the autonomous vehicle moves without slipping on a plane, that means there is a pure rolling contact between the wheels and the ground and also there is no lateral slip between the wheel and the plane. The vehicle has four differentially driven wheels placed on the vehicle platform. Electrical motors drive the back wheels independently in skidding steering system. The motion of the AGV is subject non-holonomic constraints. All wheels have the same radius ' $r$ '. The back driven wheels are separated by distance ' $2L$ '. The posture of the vehicle in a two-dimensional workspace can be defined instantaneously by the situation in Cartesian coordinates ( $x$  and  $y$ -axes) and the orientation with respect to a global frame. The configuration of the vehicle is represented by generalised coordinates,  $P_c = (X_c, Y_c, \theta)$  (Al-Mayyahi et al., 2014).

The relationships for kinematic model of the AGV can be given as in below:

$$\begin{bmatrix} v_x \\ v_y \\ \dot{\theta} \end{bmatrix} = \begin{bmatrix} \frac{r}{2} & \frac{r}{2} \\ 0 & 0 \\ \frac{r}{L} & -\frac{r}{L} \end{bmatrix} \begin{bmatrix} \omega_r \\ \omega_l \end{bmatrix} \quad (1)$$

$$v(t) = r \cdot \left[ \frac{\omega_r + \omega_l}{2} \right] \quad (2)$$

$$\dot{\theta}(t) = r \cdot \left[ \frac{\omega_r - \omega_l}{L} \right] \quad (3)$$

$$\dot{x}_c = v(t) \cos \theta \quad (4)$$

$$\dot{y}_c = v(t) \sin \theta \quad (5)$$

$$\dot{\theta}(t) = \omega \quad (6)$$

$$\omega_r = \dot{\varphi}_r \quad (7)$$

$$\omega_l = \dot{\varphi}_l \quad (8)$$

In additional, the derived model of the AGV is subject to the non-holonomic constraints. For instance, the contact between the wheels and the ground, non-slipping and finally the pure rolling (Fierro and Lewis, 1998) as in the following equations.

- No slip constraint

$$\dot{y}_c \cos \theta - \dot{x}_c \sin \theta = a \dot{\theta} \quad (9)$$

- Pure rolling constraint

$$\dot{x}_c \cos \theta + \dot{y}_c \sin \theta + L \dot{\theta} = r \dot{\varphi}_r \quad (10)$$

$$\dot{x}_c \cos \theta + \dot{y}_c \sin \theta - L \dot{\theta} = r \dot{\varphi}_l \quad (11)$$

These constraints show that the driven wheels do not slip. The three non-holonomic constraints can be written in the following form:

$$A(q) \dot{q} = 0 \quad (12)$$

$$A(q) = \begin{bmatrix} -\sin \theta & \cos \theta & -a & 0 & 0 \\ \cos \theta & \sin \theta & L & -r & 0 \\ \cos \theta & \sin \theta & -L & 0 & -r \end{bmatrix} \quad (13)$$

$$\dot{q} = [\dot{x}_c \quad \dot{y}_c \quad \dot{\theta} \quad \dot{\varphi}_r \quad \dot{\varphi}_l]^T \quad (14)$$

The aforementioned system can be re-written into a more proper representation form for governing the model and simulation of the entire system. In the new representation, the constraint terms from the equations above can be eliminated. The new representation form as in below gives the kinematic matrix:

$$\dot{q} = \begin{bmatrix} \dot{x}_c \\ \dot{y}_c \\ \dot{\theta} \\ \dot{\omega}_r \\ \dot{\omega}_l \end{bmatrix} = \begin{bmatrix} \cos\theta & -a \sin\theta \\ \sin\theta & a \cos\theta \\ 0 & 1 \\ \frac{1}{r} & \frac{L}{r} \\ \frac{1}{r} & -\frac{L}{r} \end{bmatrix} \begin{bmatrix} V \\ \omega \end{bmatrix} \quad (15)$$

where

$v_x$  the velocity of the vehicle in x-direction

$v_y$  the velocity of the vehicle in y-direction

$\theta$  moving vehicle orientation

$\omega_r$  angular velocity of right wheel

$\omega_l$  angular velocity of left wheel

$\omega$  angular velocity of vehicle.

This model is referred to a vehicle's kinematic model since it describes the velocities but not the forces or torques that have effects on the velocity.

## 2.2 Dynamic model

The dynamic model of an autonomous vehicle represents the study of the relationship between the various forces action on a robot mechanism and their accelerations. This is mainly used for simulation study and analysis of vehicle's design and a motion controller design for the vehicle. The description of the mechanism of the robot movement is given in terms of its component parts; bodies, joints and the parameters that characterise them. In fact, several parameters are required to define the dynamic model of a given rigid body such inertia, centre of mass and applied forces. The dynamic model of the AGV was derived based on energy-Lagrangian method. The equation below is described in a well-known formula (Fierro and Lewis, 1997).

$$M(q)\dot{\omega} + C(q, \dot{q})\omega + F(\dot{q}) = B(q)T \quad (16)$$

where

$M(q)$  the symmetric positive definite inertia matrix

$C(q, \dot{q})$  the centripetal and Coriolis matrix

$F(\dot{q})$  the surface friction matrix

$B(q)$  the input transformation matrix

$T$  the input vector.

The equation (16) can be rewritten in a more appropriate way as follows:

$$M(q)\dot{\omega} + C(q, \dot{q})\omega + B(q)T \quad (17)$$

The above equation represents the dynamic behaviour of the AGV. The final equation that governs the dynamic model can be written in the simplified matrix form given below:

$$\begin{bmatrix} m & 0 \\ 0 & ma^2 + I_c \end{bmatrix} \begin{bmatrix} \dot{\omega} \\ \ddot{\theta} \end{bmatrix} + \begin{bmatrix} 0 & -ma\dot{\theta} \\ ma\dot{\theta} & 0 \end{bmatrix} \begin{bmatrix} \omega \\ \dot{\theta} \end{bmatrix} = \frac{1}{r} \begin{bmatrix} 1 & 1 \\ L & -L \end{bmatrix} \begin{bmatrix} T_r \\ T_l \end{bmatrix} \quad (18)$$

The matrices elements are stated as follows:

$$M(q) = \begin{bmatrix} m & 0 \\ 0 & ma^2 + I_c \end{bmatrix} \quad (19)$$

$$C(q, \dot{q}) = \begin{bmatrix} 0 & -ma\dot{\theta} \\ ma\dot{\theta} & 0 \end{bmatrix} \quad (20)$$

$$B(q) = \frac{1}{r} \begin{bmatrix} 1 & 1 \\ L & -L \end{bmatrix} \quad (21)$$

The relevant physical parameters of the AGV are shown in Table 1.

**Table 1** The physical parameters of the AGV

Parameter	Description	Value	Unit
$r$	Wheel radius	0.1	m
$L$	The distance between the one of driven wheel and the axis of centre point	0.60	m
$a$	The distance between the centre of total mass and centre axis of the back driven wheels	0.25	m
$m$	The mass of the vehicle with driving wheels and DC motors	20	kg
$I_c$	The mass moment of inertia about the centre of mass	4	Kgm <sup>2</sup>
$d_{11}$ and $d_{22}$	Surface friction coefficients	10	Each

## 2.3 Actuation system

Consider the driving control unit of the vehicle wheel, an actuator is an electrical motor that drives a mechanical part of a robotic mechanism. The actuator receives a control signal directly from a control system to drive wheels into a specified motion. A DC motor is used as an actuator in this work. The model of DC motor is given in the following equations:

$$T_m = k_m i_a \quad (22)$$

$$v_b = k_b \omega_m \quad (23)$$

$$E = R_a i_a + L_a \frac{di_a}{dt} + v_b \quad (24)$$

$$J_m \frac{d\omega_m}{dt} + b_m \omega_m + T_L = T_m \quad (25)$$

where

$\omega_m$  = the angular speed of the motor

$i_a$  = the motor current

$E$  = the applied voltage to the motor, which is  $E_r$  for the right motor and  $E_l$  for the left one

$v_b$  = the back e.m.f. voltage

$J_m$  = the motor inertia

$T_m$  = the motor torque

$T_L$  = load torque.

The physical parameters of the actuator are given in Table 2.

**Table 2** The physical parameters of the actuator

Parameter	Description	Value	Unit
$R_a$	The resistance of the armature winding	8	$\Omega$
$L_a$	The inductance in the motor winding	0	Henry
$J_m$	The motor inertia	0	$\text{kgm}^2$
$k_m$	The torque constant	0.35	N.m/A
$k_b$	The back e.m.f. constant	0.35	V.s/rad
$b_m$	viscous friction	0	N.m.s

### 3 Fractional order systems

In this section, the generic control scheme will be explained. It can be classified mainly into three parts. Firstly, the fractional order PID controller is introduced as the first part of the concept of. Secondly, the fractional order PID controller. In recent years, researchers reported that fractional order systems for modelling various systems more adequately than conventional techniques. The fractional order systems have main effect over the controller system behaviour. For instance, to increase the speed of the response, and decrease the steady-state error and relative stability (Monje et al., 2010).

#### 3.1 Fractional order calculus

Fractional calculus is a mathematical topic which studies the ability of taking real number power of both the differential and integration operators. There are several definitions to describe the fractional derivative. The firmly established definitions are Grunwald-Letnikov definition and the Riemann-Liouville definition. The most frequently used definition in fractional-order calculus is the Riemann-Liouville definition, in which the fractional order integration is defined as follows:

$${}_a D_t^{-\beta} f(t) = \frac{1}{\Gamma(\beta)} \int_a^t (t-\tau)^{\beta-1} f(\tau) d\tau \quad (26)$$

where  $\beta$  represents the real order of the differential and integral ( $0 < \beta < 1$ );  $a$  is the initial time instance, often assumed to be zero; and  $t$  is the parameter for which both of the differential and integral are taken. The Laplace and Fourier transforms of the fractional derivative of  $f(t)$  is given by:

$$L[D_t^\beta f(t)] = S^\beta L[f(t)] - \sum_{k=1}^n S^k [D_t^{\beta-k-1} f(t)]_{t=0} \quad (27)$$

For convenience, the second part on the right hand side of equation (31) can be ignored when the derivatives of the function  $f(t)$  are all equal to 0 at  $t = 0$ . Therefore, that equation can be rewritten as in below:

$$L[D_t^\beta f(t)] = S^\beta F(s) \quad (28)$$

where  $F(s)$  is the Laplace transformer of  $f(t)$ .

#### 3.2 Fractional order PID controller

The integral-differential equation defining the control action of a fractional order PID controller is given by

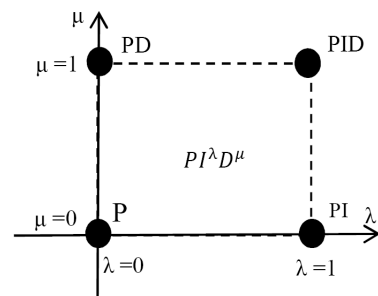
$$u(t) = K_p e(t) + K_i D^{-\lambda} e(t) + K_d D^\mu e(t) \quad (29)$$

Applying Laplace transform to equation above with null initial conditions, hence, the transfer function of the controller can be expressed by:

$$C_f(s) = K_p + \frac{K_i}{S^\lambda} + K_d S^\mu \quad (30)$$

In a graphical way, the control possibilities using a fractional-order PID controller are shown in Figure 2, extending the four control points of the classical PID to the range of control points of the quarter-plane defined by selecting the values of  $\lambda$  and  $\mu$ . Therefore, the essential advantage of the fractional order PID controller is the less sensitive to changes might happen to parameters of a controlled plant. In fact, the two extra degrees produce more adjustment for the dynamic behaviour of the fractional order PID controller than a conventional case.

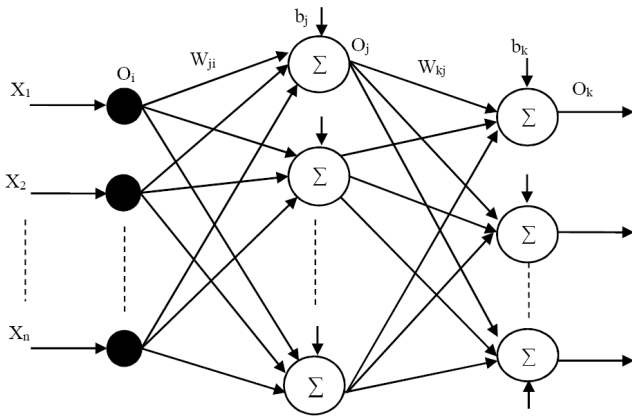
**Figure 2** Generalised FOPID controller



#### 4 Neural network architecture

Neural network architecture can be created using two or more combined neurons to form a multi-layer network. Figure 3 depicts an example of a multilayer architecture for a neural network. It is apparent that the architecture of neural network consists of three layers, i.e., input layer, hidden layer and output layer. First of all, the input layer receives variables related to a problem which has a finite number of inputs and duplicate the value to their multiple outputs. The nodes of the input layer are passive. It means that they do not modify the data. The second layer for this example is the hidden layer which processes the information between the input and output layers of the network to develop a behavioural representation of the problem. Finally, the output layer provides the desired outputs of a trained system. Individual nodes are given at the end of each layer in a neural network. These nodes emulate biological neurons by taking input data and performing simple operations on the data. The relationship between the nodes is manipulated by weights associated with nodes' outputs. This means that each node represents a summation value of all inputs that feed a particular node. Several transfer functions can be involved to manipulate the relationship between inputs and output of each node such as Sigmoid, Gaussian and so on. In addition, there are biases associated with nodes to activate it.

**Figure 3** Three layers neural network



The set of relationship for manipulating the interconnection between the layers at each stage is given below:

$$O_k = f(net_k) \quad (31)$$

$$net_k = \left( \sum_j W_{kj} O_j + b_k \right) \quad (32)$$

$$O_j = f(net_j) \quad (33)$$

$$net_j = \left( \sum_i W_{ji} O_i + b_j \right) \quad (34)$$

where

$W_{ji}$  The weights between the input layer and the hidden layer.

$W_{kj}$  The weights between the hidden layer and the output layer.

$b_j$  and  $b_k$  The biases of the hidden layer and the output layer, respectively.

$f(net)$  The transfer functions in both the hidden and output layer and can have different forms such as linear, sigmoid and hyperbolic tangent sigmoid transfer function. Transfer functions calculate a layer's output from its net input.

Different optimisations algorithms have already been developed for neural-networks training. For instance, the backpropagation (BP) algorithm that could be considered one of the most applied algorithms for training of ANNs (Wilamowski, 2009). The BP algorithm is still widely used at the present; however, the slow convergence makes this algorithm to be considered an inefficient algorithm. The two main causes of the slow convergence in BP algorithm are firstly; its step sizes until completing gradients process; and secondly the curvature of the error surface may not be the same in all directions. Gauss-Newton algorithm is introduced as new algorithm to greatly improve the slow convergence. This algorithm is based on second-order derivatives of an error function to assess the error in the curvature surface in contrast with BP algorithm which is based on first order derivative.

The step size in the Gauss-Newton algorithm can be found for each direction which will converge very fast. In particular, if the error function has a quadratic surface. However, there is still a problem might happen if the quadratic approximation of error function is not reasonable. This in turn will lead the Gauss-Newton algorithm to be mostly divergent (Yu and Bogdan, 2011). Therefore, the LM is introduced due to its benefits over the BP and Gauss-Newton algorithms. LM algorithm is a combination of BP algorithm and Gauss-Newton algorithm. In LM algorithm a numerical solution is provided to a problem for minimising a nonlinear function. Moreover, it is fast and has stable convergence and it is suitable for training small- and medium-sized problems. Where, it inherits the stability of the BP algorithm and the speed advantage of the Gauss-Newton algorithm. To fully understand the derivation of the LM algorithm, the following four training algorithms will be presented; beginning with:

- 1 back-propagation algorithm
- 2 Newton's method
- 3 Gauss-Newton's algorithm
- 4 ending with LM algorithm.

The mean square error (MSE) is defined in equation below to evaluate the error value in training process. It is calculated for all training process and network outputs as follows:

$$E(x, w) = \frac{1}{2} \sum_{p=1}^P \sum_{m=1}^M e_{p,m}^2 \quad (35)$$





From the equation above, it is obvious that there are  $N$  parameters for  $N$  equations. This means all  $\Delta w_i$  can be calculated during the learning process, the weights will be updated iteratively. Equation (44) can be written in a matrix form as in follows:

$$\begin{bmatrix} -g_1 \\ -g_2 \\ \dots \\ -g_N \end{bmatrix} = \begin{bmatrix} -\frac{\partial E}{\partial w_1} \\ -\frac{\partial E}{\partial w_2} \\ \dots \\ -\frac{\partial E}{\partial w_N} \end{bmatrix} \quad (45)$$

$$= \begin{bmatrix} \frac{\partial^2 E}{\partial w_1^2} & \frac{\partial^2 E}{\partial w_1 \partial w_2} & \dots & \frac{\partial^2 E}{\partial w_1 \partial w_N} \\ \frac{\partial^2 E}{\partial w_2 \partial w_1} & \frac{\partial^2 E}{\partial w_2^2} & \dots & \frac{\partial^2 E}{\partial w_2 \partial w_N} \\ \dots & \dots & \dots & \dots \\ \frac{\partial^2 E}{\partial w_N \partial w_1} & \frac{\partial^2 E}{\partial w_N \partial w_2} & \dots & \frac{\partial^2 E}{\partial w_N^2} \end{bmatrix} \times \begin{bmatrix} \Delta w_1 \\ \Delta w_2 \\ \dots \\ \Delta w_N \end{bmatrix}$$

where the square matrix is Hessian matrix:

$$H = \begin{bmatrix} \frac{\partial^2 E}{\partial w_1^2} & \frac{\partial^2 E}{\partial w_1 \partial w_2} & \dots & \frac{\partial^2 E}{\partial w_1 \partial w_N} \\ \frac{\partial^2 E}{\partial w_2 \partial w_1} & \frac{\partial^2 E}{\partial w_2^2} & \dots & \frac{\partial^2 E}{\partial w_2 \partial w_N} \\ \dots & \dots & \dots & \dots \\ \frac{\partial^2 E}{\partial w_N \partial w_1} & \frac{\partial^2 E}{\partial w_N \partial w_2} & \dots & \frac{\partial^2 E}{\partial w_N^2} \end{bmatrix} \quad (46)$$

By combining equations (37) and (45) with equation (46)

$$-g = H \Delta w \quad (47)$$

Thus,

$$\Delta w = -H^{-1} g \quad (48)$$

Therefore, in Newton's method, the incremental updating rule for weights is given below:

$$w_{k+1} = w_k - H_k^{-1} g_k \quad (49)$$

$H$  is defined as a Hessian matrix that provides the second-order derivatives of total error function and gives the proper evaluation on the change of gradient descent.

### 4.3 Gauss-Newton algorithm

In Gauss-Newton algorithm, Jacobian matrix  $J$  is introduced to simplify the calculation process due to the complexity inherited the second-order derivatives of total error function with Newton's method.

$$J = \begin{bmatrix} \frac{\partial e_{1,1}}{\partial w_1} & \frac{\partial e_{1,1}}{\partial w_2} & \dots & \frac{\partial e_{1,1}}{\partial w_N} \\ \frac{\partial e_{1,2}}{\partial w_1} & \frac{\partial e_{1,2}}{\partial w_2} & \dots & \frac{\partial e_{1,2}}{\partial w_N} \\ \dots & \dots & \dots & \dots \\ \frac{\partial e_{1,M}}{\partial w_1} & \frac{\partial e_{1,M}}{\partial w_2} & \dots & \frac{\partial e_{1,M}}{\partial w_N} \\ \dots & \dots & \dots & \dots \\ \frac{\partial e_{p,1}}{\partial w_1} & \frac{\partial e_{p,1}}{\partial w_2} & \dots & \frac{\partial e_{p,1}}{\partial w_N} \\ \frac{\partial e_{p,2}}{\partial w_1} & \frac{\partial e_{p,2}}{\partial w_2} & \dots & \frac{\partial e_{p,2}}{\partial w_N} \\ \dots & \dots & \dots & \dots \\ \frac{\partial e_{p,m}}{\partial w_1} & \frac{\partial e_{p,m}}{\partial w_2} & \dots & \frac{\partial e_{p,m}}{\partial w_N} \end{bmatrix} \quad (50)$$

By integrating equations (35) and (37), gradient descent's elements can be calculated as follows:

$$g_i = \frac{\partial E}{\partial w_i} = \frac{\partial \left( \frac{1}{2} \sum_{p=1}^p \sum_{m=1}^m e_{p,m}^2 \right)}{\partial w_i} \quad (51)$$

$$= \sum_{p=1}^p \sum_{m=1}^m \left( \frac{\partial e_{p,m}}{\partial w_i} e_{p,m} \right)$$

Combining equations (50) and (51), the relationship between gradient descent ( $g$ ) and Jacobian matrix ( $J$ ) and would be

$$g = J e \quad (52)$$

where the error ( $e$ ) has the following form;

$$e = \begin{bmatrix} e_{1,1} \\ e_{1,2} \\ \dots \\ e_{1,m} \\ \dots \\ e_{p,1} \\ e_{p,2} \\ \dots \\ e_{p,m} \end{bmatrix} \quad (53)$$

Inserting equation (35) into (36), the elements of Hessian matrix, i.e.,  $i^{\text{th}}$  row and  $j^{\text{th}}$  column can be calculated as

$$h_{i,j} = \frac{\partial^2 E}{\partial w_i \partial w_j} = \frac{\partial^2 \left( \frac{1}{2} \sum_{p=1}^p \sum_{m=1}^m e_{p,m}^2 \right)}{\partial w_i \partial w_j} \quad (54)$$

$$= \sum_{p=1}^p \sum_{m=1}^m \frac{\partial e_{p,m}}{\partial w_i} \frac{\partial e_{p,m}}{\partial w_j} + S_{i,j}$$

where  $S_{i,j}$  is equal to

$$S_{i,j} = \sum_{p=1}^p \sum_{m=1}^m \frac{\partial^2 e_{p,m}}{\partial w_i \partial w_j} e_{p,m} \quad (55)$$

From Newton's method, it is assumed that the  $S_{i,j}$  is closed to zero. Therefore, the relationship between Jacobian matrix ( $J$ ) and Hessian matrix ( $H$ ) can be rewritten as follow:

$$H \approx J^T J \quad (56)$$

By combining equations (49), (52) and (56), the weights updating rule of the Gauss-Newton algorithm can be given as in below:

$$w_{k+1} = w_k - (J_k^T J_k)^{-1} J_k e_k \quad (57)$$

#### 4.4 LM algorithm

This algorithm is an approximation to Newton's method (Hagan and Menhaj, 1994). In order to make sure that the approximated Hessian matrix is invertible, LM algorithm introduces another approximation to Hessian matrix as follows:

$$H \approx J^T J + \mu I \quad (58)$$

where

$\mu$  combination coefficient and it is always positive,

$I$  the identity matrix.

By combining equations (57) and (58), the update rule for weights of LM algorithm can be obtained as follows:

$$w_{k+1} = w_k - (J_k^T J_k + \mu I)^{-1} J_k e_k \quad (59)$$

The LM algorithm switches between the two BP algorithms and the Gauss-Newton algorithm during the training process. Two situations will be considered in LM algorithm. Firstly, if the combination coefficient ( $\mu$ ) is very small, hence, equation (59) is approaching to equation (57) and Gauss-Newton algorithm is used. However, if combination coefficient ( $\mu$ ) is very large, equation (59) approximates to equation (38) and the BP algorithm is used.

The following steps describe the training process of LM algorithms:

Step 1 Generate the initial weights.

Step 2 update weights using equation (59).

Step 3 Evaluate the error at each updated weights.

Step 4 If the new error is increased after updating, go to Step 2 and try an update again after increasing combination coefficient  $\mu$  by a suitable factor. Otherwise, go to Step 5.

Step 5 If the new error is decreased, then, compare the new error with the required value. If the new error is smaller than the required value, then, stop learning. Otherwise, go to Step 2.

Table 3 summarises the update rules for various algorithms.

## 5 Trajectory tracking control scheme of AGV

The implementation process of the entire control scheme of the ANN and the AGV model can be classified into three parts. The first one is depicted in Figure 4 that represents the relationship between a FOPID-NN controller and a plant. The second part is represented by Figure 5 which shows the training phase for a model. The optimal values of the trainable parameters of the neural controller are met using MSE cost function. The entire control scheme is depicted in Figure 6. Two trained neural network controllers are used for driving the right and left motor voltage of the vehicle separately to enable the AGV of tracking a predefined trajectory. The first controller receives the error between the desired generated trajectory and actual trajectory in order to control the ordination angle of the AGV. Therefore, the vehicle must change its orientation as needed to track the desired trajectory. The output of this controller is directly connected to the right motor voltage. The second controller utilises the error signal between the desired and actual velocity as an input. The desired velocity is assumed to a constant during the tracking process. The output of this controller is fed to the left motor voltage of the AGV. The main purpose of the second controller is to maintain a constant velocity for controlling the motion. The input and output data obtained from the FOPID controller that implemented in an earlier work are used to train the parameters of neural controller using the LM training algorithm.

**Table 3** Specifications of various algorithms

Algorithms	Update rules	Convergence	Computation complexity
BP algorithm	$w_{k+1} = w_k - \alpha g_k$	Stable, slow	Gradient
Newton algorithm	$w_{k+1} = w_k - H_k^{-1} g_k$	Unstable, fast	Gradient and Hessian
Gauss-Newton algorithm	$w_{k+1} = w_k - (J_k^T J_k)^{-1} J_k e_k$	Unstable, fast	Jacobian
Levenberg-Marquardt algorithm	$w_{k+1} = w_k - (J_k^T J_k + \mu I)^{-1} J_k e_k$	stable, fast	Jacobian

Figure 4 The neural network of one part of AGV model

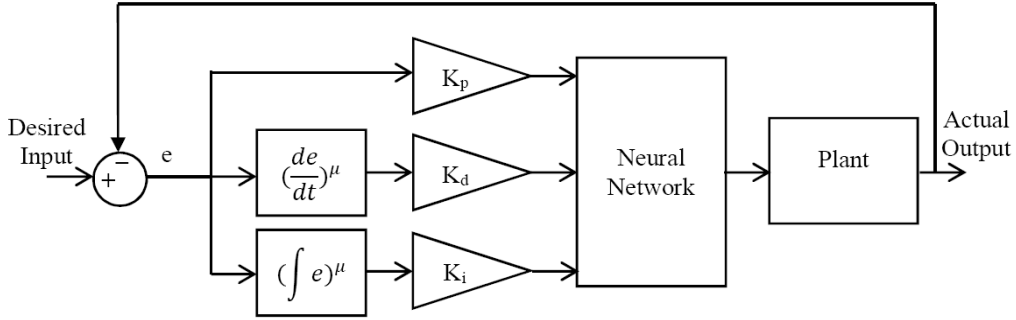


Figure 5 The training phase of the neural controller

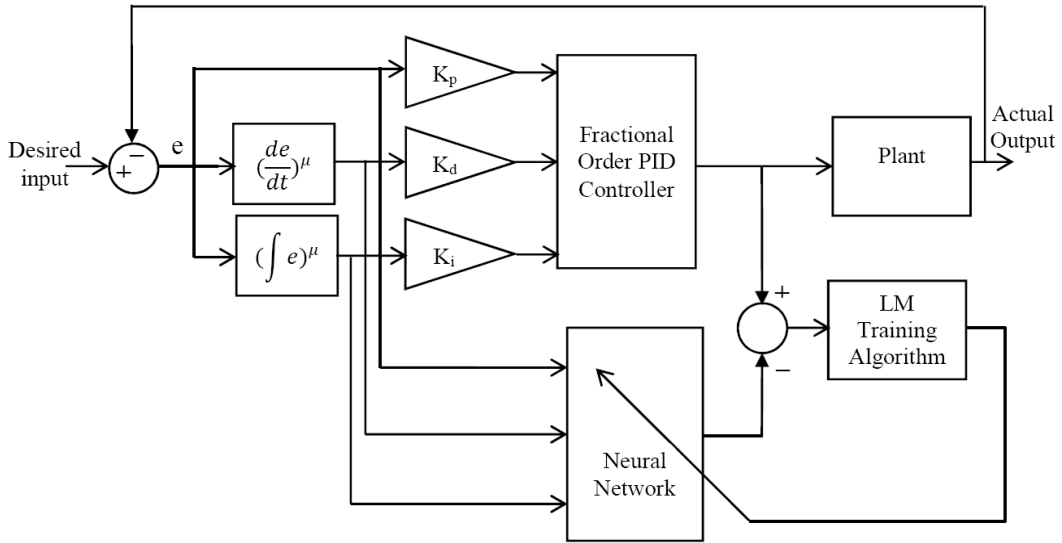
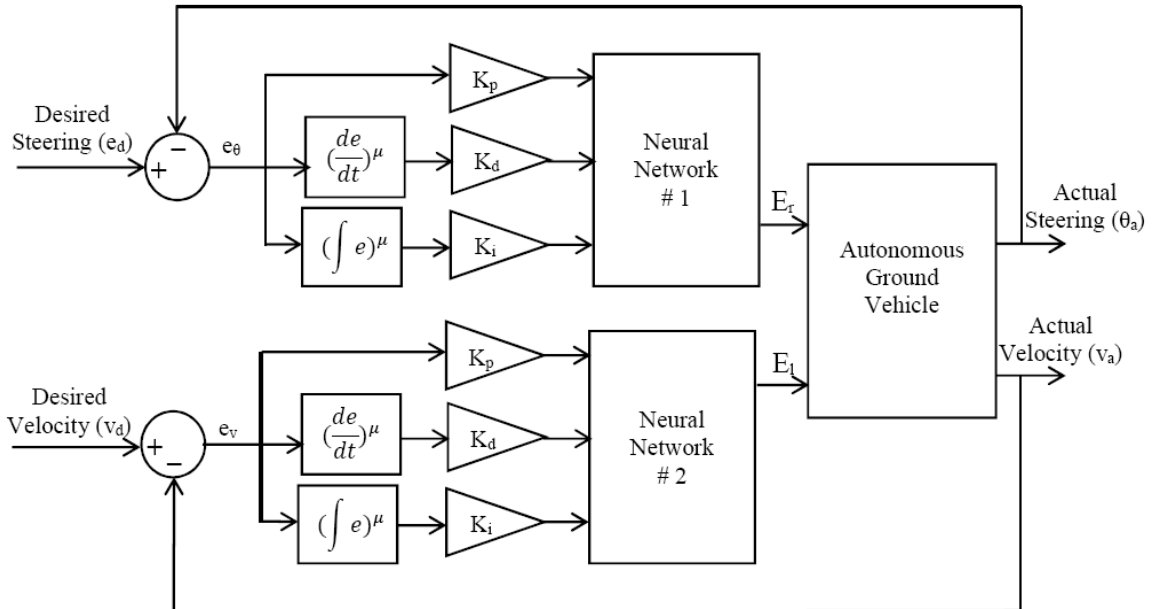


Figure 6 The block diagram of the control structure



The tracking orientation error and tracking velocity error are measured by using equations below respectively:

$$e_{\theta}(t) = \theta_d(t) - \theta_a(t) \quad (60)$$

$$e_v(t) = v_d(t) - v_a(t) \quad (61)$$

where  $\theta_d(t)$  = the desired orientation angle,  $\theta_a(t)$  = the actual orientation angle,  $e_{\theta}(t)$  = the tracking orientation error,

$v_r(t)$  = the desired velocity,  $v_a(t)$  = the actual velocity, and  $e_v(t)$  = tracking velocity error.

**Figure 7** Training performance for NN of orientation tracking control (see online version for colours)

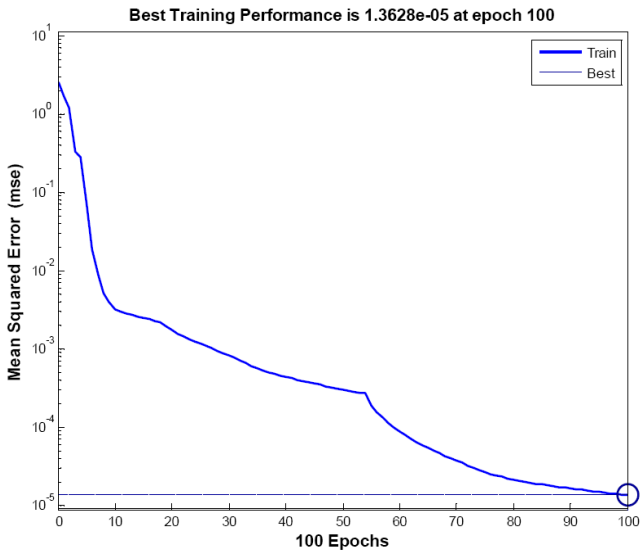
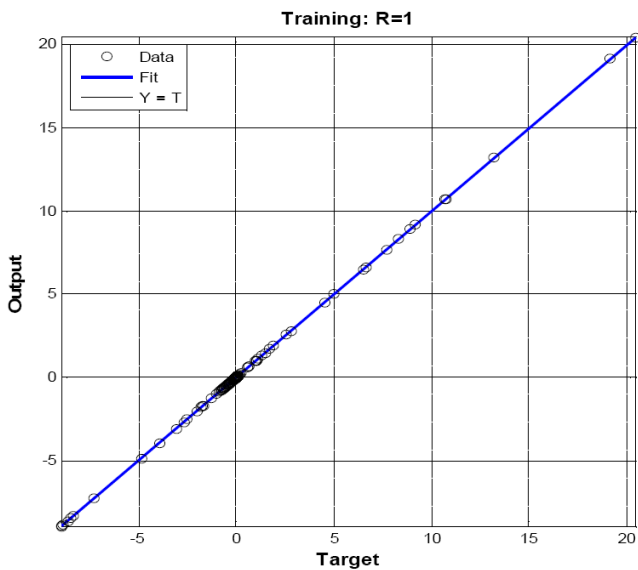


**Figure 8** Regression plot for NN of orientation tracking control (see online version for colours)



The parameters of neural network # 1 are discussed as follows: the number of neuron in the hidden layer is seven. The type of a transfer function used in the hidden layer is hyperbolic tangent sigmoid transfer function. It means that the number of biases in hidden layer is seven, and the number of weights between the input layer and the hidden layer is 21. Because there is only one output for each NN controller, it means the numbers of weights between the hidden layer and the output layer is seven and we have only one bias in the output layer. Linear transfer function is used in the output layer. The weights and biases of this network are given below. The performance progress of training against epoch numbers is depicted in Figure 7. It is apparently that mean squared error equals  $7.1133e-05$  which

is the minimum average squared error and the best training performance obtained between outputs and targets. The dashed line is the best goal which equals  $1e-05$  as set in the MATLAB code. In Figure 8, the dashed line represents the perfect result (outputs = targets). The solid line represents the best fit linear regression between outputs and targets. The 'R' value is an indication of the relationship between the outputs and targets. If 'R' = 1, this indicates that there is an exact linear relationship between outputs and targets. If 'R' is close to zero, there is no linear relationship between outputs and targets. We notice that 'R' = 1 which is indicated the exact linear relationship as intended.

$$weights1 = \begin{bmatrix} -0.1057 & -0.085 & -0.1008 \\ 2.0921 & -0.1116 & 0.0255 \\ -0.1352 & -0.1311 & -0.1392 \\ -0.4273 & 0.5521 & -1.0398 \\ -0.1101 & -0.1114 & -0.1095 \\ -0.9518 & 1.0621 & 1.1808 \\ -0.4648 & -0.4036 & -0.4663 \end{bmatrix},$$

$$biases1 = \begin{bmatrix} 1.6743 \\ 4.8324 \\ 0.4940 \\ 0.3517 \\ -0.6441 \\ 1.4443 \\ -4.4652 \end{bmatrix}$$

$$weights2 = \begin{bmatrix} -9.1761 & 0.0020 & -3.3567 & 0.0024 \\ -6.9362 & 0.0016 & -1.7127, \end{bmatrix}$$

$$biases2 = [4.4342]$$

In the similar way, the parameters of neural network # 2 stated that the best training performance (mean squared error equals) is  $2.3545e-05$  as depicted in Figure 9. In this network, the number of neurons in the hidden layer is ten. Linear and hyperbolic tangent sigmoid transfer functions are used in the hidden and output layers, respectively. In Figure 10, we also noticed that 'R' = 1 which is indicated the exact linear relationship as targeted. The weights and biases of this network are given below:

$$weights1 = \begin{bmatrix} -0.0585 & 0 & -2.666 \\ 0.6865 & 0 & 1.8055 \\ -2.0203 & 0 & 2.8419 \\ 0.0777 & 0 & 0.1210 \\ -0.0607 & 0 & -0.9775 \\ -0.8962 & 0 & -2.0130 \\ -1.4326 & 0 & 0.4341 \\ -1.199 & 0 & -1.1419 \\ 0.0095 & 0 & 0.0396 \\ -3.866 & 0 & -3.9976 \end{bmatrix},$$

$$biases1 = \begin{bmatrix} 4.808 \\ 3.134 \\ 7.407 \\ -5.789 \\ -3.565 \\ -3.179 \\ -3.458 \\ -2.550 \\ 0.427 \\ 7.531 \end{bmatrix}$$

$$weights2 = \begin{bmatrix} -15.55 & -1.676 & -18.58 & 36.65 & 9.25 \\ -14.34 & -16.79 & -13.26 & 13.39 & -15.40 \end{bmatrix}$$

$$biases2 = [2.405]$$

**Figure 9** Training performance for NN of velocity tracking control (see online version for colours)

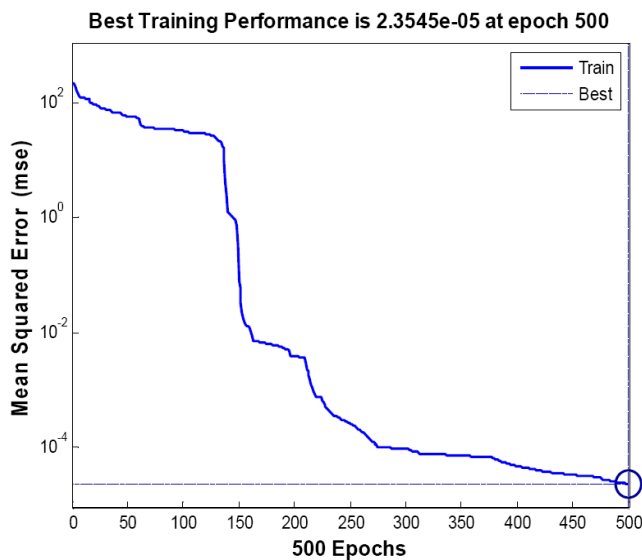
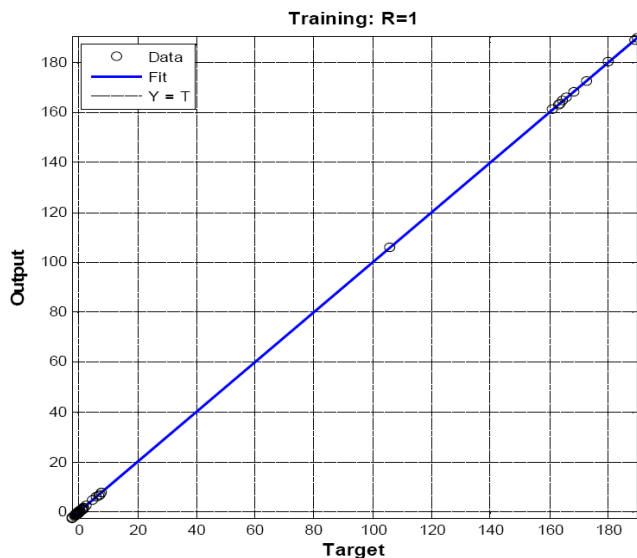


**Figure 10** Regression plot for NN of velocity tracking control (see online version for colours)



## 6 Simulation results

The implementation of neural network controller is carried out using MATLAB-Simulink. A circular trajectory is generated as a reference fed into the control system and the latter is simulated to demonstrate the effectiveness and performance of the proposed architecture shown in Figure 4 aforementioned. The simulation experiments are conducted to track the desired the orientation and velocity of the AGV. The introduced neural network controller is trained online by LM algorithm. For the simulation purpose, the desired velocity and the desired orientation angle are taken as  $v_d = 0.25$  m/s and  $\theta_d(t) = [(2\pi * t) / -40]$  rad, respectively. The simulation results for the circular trajectory are conducted for the interval  $t \in [0, 40]$ . Figure 11 shows that the AGV tracking the desired trajectory and the corresponding actual trajectory using FOPID and NN controllers. In Figures 12(a) and 12(b), the simulation results obtained from NN controller show that the error of linear velocity and orientation angle converge faster to the corresponding desired velocity and orientation angle respectively by comparison with FOPID. Figures 13(a) and 13(b) show the motion trajectory of the AGV in the motion control in both X and Y coordinates. As can be seen from these figures, the AGV immediately heads towards the desired velocity and orientation angle that is moving on the circle. It then reaches them quickly and continues to track them. In the meantime, the tracking control is reasonably accurate owing to the quick online learning and adaptive capability of the ANNs. The simulation results demonstrate that the adaptive control of the ANN for the AGV is capable of better tracking performance in comparison to FOPID.

**Figure 11** The generated desired circular and the actual trajectories (see online version for colours)

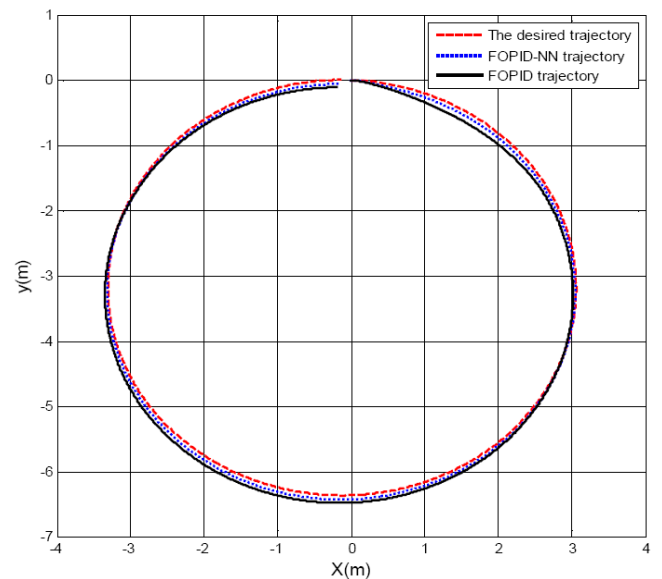
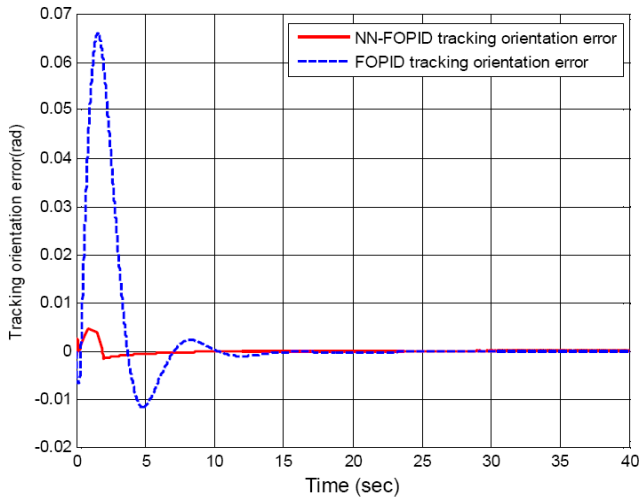
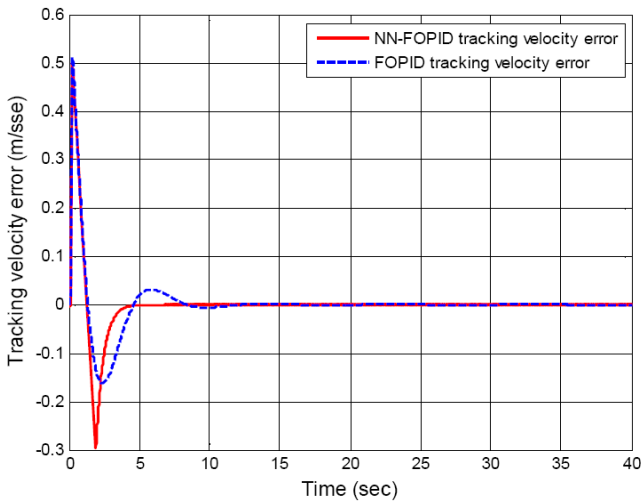


**Figure 12** The tracking error of (a) vehicle velocity (b) orientation angle (see online version for colours)

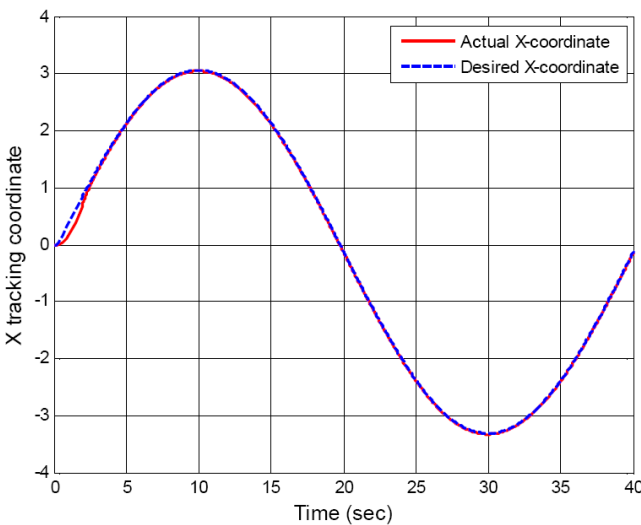


(a)



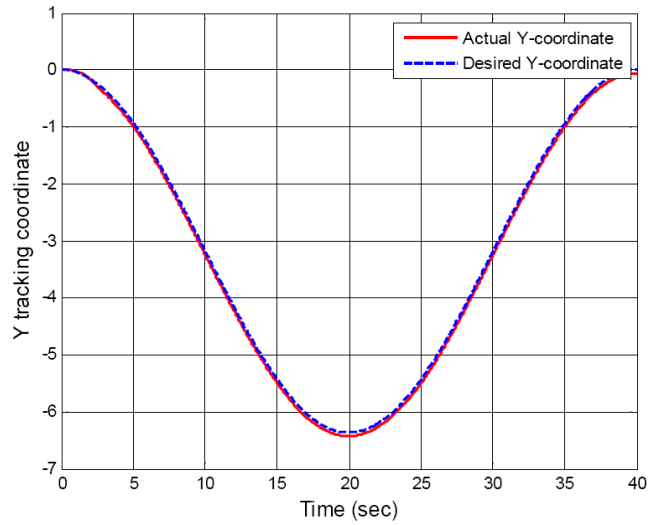
(b)

**Figure 13** The desired and actual coordinates (a) X-axis tracking and (b) Y-axis tracking (see online version for colours)



(a)

**Figure 13** The desired and actual coordinates (a) X-axis tracking and (b) Y-axis tracking (continued) (see online version for colours)



(b)

## 7 Conclusions

A neural network based on a  $PI^{\lambda}D^{\mu}$  controller has been introduced to control AGV motion. The LM algorithm was used to train the parameters of the neural network controller. The designed neural network controller has shown more accurate capability to track the desired circular trajectory in comparison to FOPID. Moreover, the neural network showed a fast learning capability to track the continuous circular trajectory. The results have confirmed successfully the effectiveness and validation of the introduced neural network controller in term of minimising the tracking error, thereby, in comparing the figures. It is obvious that the smoothness and faster convergence performance of error tracking for the vehicle velocity and orientation angle.

## Acknowledgements

The authors thank the Ministry of Higher Education and Scientific Research in Iraq for funding this research work in the UK. The authors also thank the home university of the first author, University of Basrah in Iraq, for the support.

## References

- Al-Mayyahi, A., Wang, W. and Birch, P. (2014) 'Adaptive neuro-fuzzy technique for autonomous ground vehicle navigation', *Robotics*, November, Vol. 3, No. 4, pp.349–370.
- Al-Mayyahi, A., Wang, W. and Birch, P. (2015) 'Path tracking of autonomous ground vehicle based on fractional order PID controller optimized by PSO', *13th IEEE Int. Symp. Appl. Mach. Intell. Informatics*, January, pp.109–114.
- Antonelli, G., Member, S., Chiaverini, S. and Fusco, G. (2007) 'A fuzzy-logic-based approach for mobile robot path tracking', *IEEE Trans. Fuzzy Syst.*, Vol. 15, No. 2, pp.211–221.

- Fierro, R. and Lewis, F.L. (1997) 'Control of a nonholonomic mobile robot: backstepping kinematics into dynamics', *J. Robot. Syst.*, Vol. 14, No. 3, pp.149–163.
- Fierro, R. and Lewis, F.L. (1998) 'Control of a nonholonomic mobile robot using neural networks', *IEEE Trans. Neural Networks*, January, Vol. 9, No. 4, pp.589–600.
- Fukao, T., Nakagawa, H. and Adachi, N. (2000) 'Adaptive tracking control of a nonholonomic mobile robot', *IEEE Trans. Robot. Autom.*, Vol. 16, No. 5, pp.609–615.
- Guo, L., Ge, P-S., Yue, M. and Zhao, Y-B. (2014) 'Lane changing trajectory planning and tracking controller design for intelligent vehicle running on curved road', *Math. Probl. Eng.*, pp.1–9.
- Hagan, M.T. and Menhaj, M.B. (1994) 'Training feedforward networks with the Marquardt algorithm', *IEEE Trans. Neural Networks*, Vol. 5, No. 6, pp.2–6.
- Hao, Y.U., Gong-you, T., Hao, S.U., Chun-peng, T. and Jian, Z. (2014) 'Trajectory tracking control of wheeled mobile robots via fuzzy approach', in *33rd Chinese Control Conference (CCC)*, pp.8444–8449.
- Jiang, Z-P. and Nijmeijer, H. (1997) 'Tracking control of mobile robots: a case study in backstepping', *Automatica*, Vol. 33, No. 97, pp.1393–1399.
- Keighobadi, J., Menhaj, M.B. and Kabgani, M. (2010) 'Feedback-linearization and fuzzy controllers for trajectory tracking of wheeled mobile robots', *Kybernetes*, March, Vol. 39, No. 1, pp.83–106.
- Liang, Y., Xu, L., Wei, R. and Hu, H. (2010) 'Adaptive fuzzy control for trajectory tracking of mobile robot', in *The IEEE International Conference on Intelligent Robots and Systems*, pp.4755–4760.
- Monje, C.A., Chen, Y., Vinagre, B.M., Xue, D. and Feliu, V. (2010) *Fractional-order Systems and Controls Fundamentals and Applications*, p.430, Springer London Dordrecht Heidelberg, New York.
- Padhy, P.K., Sasaki, T., Nakamura, S. and Hashimoto, H. (2010) 'Modeling and position control of mobile robot', *11th IEEE Int. Work. Adv. Motion Control*, March, pp.100–105.
- Pawlowski, S., Dutkiewicz, P., Kozłowski, K. and Wroblewski, W. (2001) 'Fuzzy logic implementation in mobile robot control', *Proc. 2nd Int. Work. Robot Motion Control. RoMoCo'01*, IEEE Cat. No. 01EX535, No. 8, pp.65–70.
- Shojaei, K., Tarakameh, A. and Shahri, A.M. (2009) 'Adaptive trajectory tracking of WMRs based on feedback linearization technique', in *IEEE International Conference on Mechatronics and Automation*, pp.729–734.
- Solea, R., Filipescu, A. and Nunes, U. (2009) 'Sliding-mode control for trajectory-tracking of a wheeled mobile robot in presence of uncertainties', in *IEEE Asian Control Conference (ACC)*, pp.1701–1706.
- Wilamowski, B.M. (2009) 'Neural network architectures and learning algorithms', *IEEE Ind. Electron. Mag.*, Vol. 3, No. 4, pp.56–63.
- Xie, M., Li, L. and Wang, Z. (2012) 'Trajectory tracking control for mobile robot based on the fuzzy sliding mode', *Proc. 10th World Congr. Intell. Control Autom.*, July, pp.2706–2709.
- Xu, Q., Kan, J., Chen, S. and Yan, S. (2014) 'Fuzzy PID based trajectory tracking control of mobile robot and its simulation in Simulink', *Int. J. Control Autom.*, August, Vol. 7, No. 8, pp.233–244.
- Ye, J. (2008) 'Adaptive control of nonlinear PID-based analog neural networks for a nonholonomic mobile robot', *Neurocomputing*, March, Vol. 71, Nos. 7–9, pp.1561–1565.
- Ye, J. (2013) 'Tracking control of two-wheel driven mobile robot using compound sine function neural networks', *Conn. Sci.*, June, Vol. 25, Nos. 2–3, pp.139–150.
- Yu, H. and Bogdan, M. (2011) 'Levenberg-Marquardt training', in *Electrical Engineering Handbook: Intelligent Systems*, pp.12/1–12/16.